

Spontaneous Oscillations in Mechanosensory Hair Bundles

Björn Nadrowski^a, Pascal Martin^b and Frank Jülicher^a

^aMax Planck Institute for the Physics of Complex Systems, Nöthnitzerstr. 38, 01187 Dresden, Germany

^bPhysicochimie Curie, Institut Curie, 26 rue d'Ulm, 75248 Paris Cedex 05, France

ABSTRACT

The ear relies on nonlinear amplification to enhance its sensitivity and frequency selectivity. It has been suggested that this active process results from dynamical systems which oscillate spontaneously. In the bullfrog sacculus, hair bundles, which are the mechanosensitive elements of sensory hair cells display noisy oscillations. These oscillations can be described in a simple model which takes into account the properties of mechanosensitive ion channels coupled to motor proteins which are regulated by inflowing Ca^{2+} ions. The role of fluctuations can be studied by adding random forcing terms with characteristic amplitudes that result from the number and properties of ion channels and motor molecules. This description can account quantitatively for the experimentally measured linear and nonlinear response functions and reveals the relevance of fluctuations for signal detection.

1. INTRODUCTION

Detecting sounds from the outside world imposes stringent demands on the design of the inner ear, where acoustic stimuli are transduced to electrical signals.¹ The vertebrate ear contains highly specialized cells called hair cells, which act as mechanosensors.² Each of these cells is responsive to a particular frequency component of the auditory input. In order to achieve high sensitivity and frequency selectivity, non-linear amplification is necessary. Because of the viscous damping at microscopic scales, the familiar resonant gain of a passive system is far from sufficient for the required demands.³

The ear relies on active systems to achieve exquisite sensitivity and sharp frequency selectivity.³⁻⁵ The most striking evidence for active behaviors in the ear are so-called otoacoustic emissions which are sounds emitted from the ears of mammals, birds and amphibians.⁶ It has recently been proposed that the ear contains active dynamical systems which are close to an oscillating instability or Hopf-bifurcation.⁷⁻⁹ This concept can explain many of the observed features of the ear, in particular, the nonlinearities that are generally observed at resonance conditions,¹⁰ the interference effects of multiple frequencies¹¹ as well as the occurrence of spontaneous emissions.

Although the cellular mechanisms that mediate this active process have remained elusive, *in vitro*¹²⁻¹⁴ as well as *in vivo*¹⁵ experiments have revealed that the mechanosensory organelle of the hair cell - the hair bundle - can generate active oscillatory movements that might underlie frequency-selective amplification. The observed noisy oscillatory system exhibits the signature of a system near a Hopf bifurcation: The response to periodic stimuli was nonlinear for sufficiently large amplitudes near the oscillation frequency.¹⁶ For small amplitudes there was a linear response regime which exhibited stable behaviors. Comparing the linear response to the autocorrelation function it was shown that the fluctuation dissipation theorem is violated, indicating the activity of the system.¹³

The hair bundles of vertebrate hair cells consist of about 50 stereocilia which are stiff, rod-like extensions of the cell with a length of several micron and a diameter of about 300nm, see Fig. 1.⁵ The stereocilia merge at the tip and are grouped in a bundle. Fine filaments, so-called tip-links form bridges between neighboring stereocilia.¹⁷ The micromechanical properties of hair bundles in living hair cells can be rich and range from adaptive movements in response to abrupt force steps with both fast and slow components,¹⁸ to spontaneous oscillations.^{5, 12, 16, 19}

Oscillatory instabilities of the hair bundle can be generated by at least three active mechanisms. First, a collection of molecular motors with a region of negative slope in the force-velocity relation becomes self oscillatory when the motor assembly is coupled to an elastic element.²⁰ In the hair bundle, the myosin-based adaptation motors in the stereocilia (reviewed in²¹) as well as the dynein motors in the kinocilium⁸ could provide such an instance. Second, coupling Ca^{2+} -mediated reclosure of the transduction channels^{18, 22-24} with gating kinetics⁷

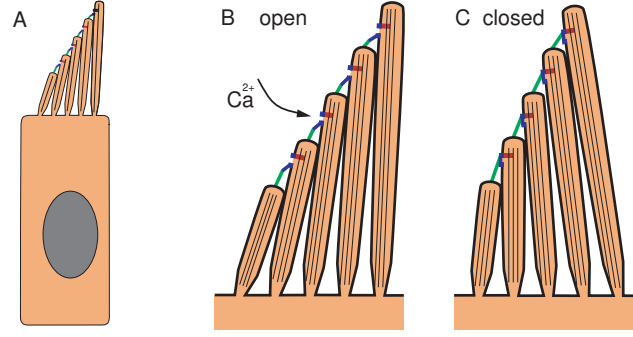


Figure 1. (A) Schematic representation of a hair cell with nucleus (grey) and a hair bundle of stereocilia which is the sensitive element of mechanosensory hair cells. It consists of 30-300 rod-like stereocilia which have a length of 1-10 μm and are connected by fine filaments, called tip-links (green). The stereocilia contain mechanosensitive ion channels which open as a result of mechanical stimulation (blue). Myosin motor molecules control the tension in the tip-links (red). (B) open and (C) closed states of a hair bundle.

or intracellular Ca^{2+} dynamics²⁵ can yield hair-bundle oscillations. Finally, the interplay between negative hair-bundle stiffness and the Ca^{2+} -dependent activity of the adaptation motors can generate oscillations.^{26, 27} This third mechanism provides the most convincing description of the hair-bundle oscillations observed in the bullfrog's sacculus and leads to a quantitative description of observed hair bundle movements and mechanical properties.²⁸

2. ACTIVE HAIR BUNDLE MECHANICS

The dynamic behavior of the hair bundle can be described by three coupled equations:

$$\lambda \dot{X} = -K_{gs}(X - X_a - DP_o) - K_{sp}X + F_{ext} + \eta \quad , \quad (1)$$

$$\lambda_a \dot{X}_a = K_{gs}(X - X_a - DP_o) - \gamma N_a f p(C) + \eta_a \quad , \quad (2)$$

$$\tau \dot{C} = C_0 - C + C_M P_o + \delta c \quad . \quad (3)$$

Eq. 1 describes the dynamics of the hair-bundle position X subjected to an external force F_{ext} . The hair bundle is subjected to friction, characterized by the coefficient λ , as well as to the elastic forces $-K_{sp}X$ and $-K_{gs}Y$, where K_{sp} and K_{gs} are the stiffnesses of stereociliary pivots and of the tip-links, respectively, with $Y = X - X_a - DP_o$. Channels are open with probability P_o and channel opening is associated with a change of the length of the tip link by distance D . Active hair-bundle movements result from forces exerted by a collection of N_a molecular motors within the hair bundle. By adjusting the gating-spring extension, these motors mediate mechanical adaptation to sustained stimuli (reviewed in²¹). The variable X_a can be interpreted as the position of the motor collection. Eq. 2 describes the mechanics and the dynamics of these motors by a linear force-velocity relation of the form $\lambda_a dX_a/dt = -F_0 + F_{mot}$, where λ_a characterizes the slope of the force-velocity relation. In the hair bundle, the motors experience an elastic force $F_{mot} = K_{gs}Y$. At stall, these motors produce an average force $F_0 = N_a \gamma f p$ that is proportional to the force f generated by a single motor and to the probability p that a motor is bound to an actin filament, where $\gamma \simeq 1/7$ is a geometric projection factor. Because adaptation depends on the Ca^{2+} concentration C , we set $p = p_0 + p_1 C$. Active force production by the motors corresponds to motors climbing up the stereocilia, i.e. $dX_a/dt < 0$, which tends to increase the extension of the gating springs and to open transduction channels. In a two-state model for channel gating,²⁹ the open probability can be written as

$$P_o = \frac{1}{1 + A e^{-(X - X_a)/\delta}} \quad , \quad (4)$$

where $A = \exp([\Delta G + (K_{gs}D^2)/(2N)]/k_B T)$ accounts for the intrinsic energy difference ΔG between the open and the closed states of a transduction channel and $\delta = N k_B T / (K_{gs}D)$.

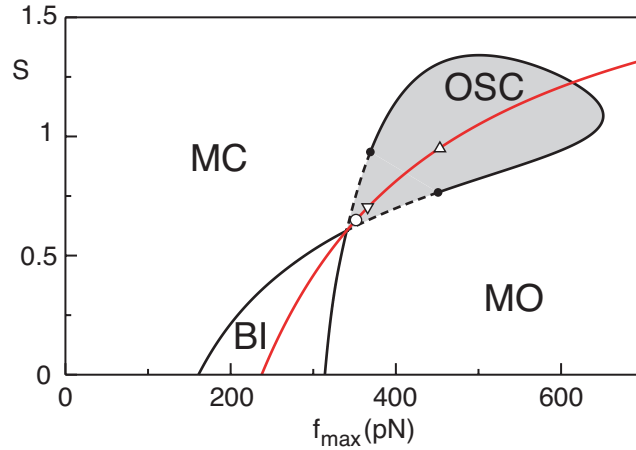


Figure 2. State diagram of the active hair bundle as a function of two control parameter, the maximal motor force f_{\max} in the absence of Ca^{2+} and the strength S of the Ca-feedback. The diagram reveals several regions: MO monostable with open channels; MC monostable with closed channels; BI bistable and oscillations (OSC). Along the red line, the open probability of ion channels is $P_o = 0.5$.

3. STATE DIAGRAM

To explore the dynamic behaviors of the system described by Eqns. 1-3, we first ignore the effects of fluctuations and assume $F_{\text{ext}} = 0$. Steady states satisfy $dX/dt = 0$, $dX_a/dt = 0$ and $dC/dt = 0$. Linear stability analysis of these steady states reveals conditions for stability as well as for oscillating instabilities that lead to spontaneous oscillations via a Hopf bifurcation.³⁰ Because calcium dynamics at the motor site is expected to be much faster than the hair-bundle oscillations observed in the bullfrog's sacculus,³¹ we determine the state diagram for $\tau = 0$ (Fig.2). The state diagram is a function of two parameters: the maximal force $f_{\max} = N_a f p_0$ produced by adaptation motors along their axis of movement, and the dimensionless feedback strength S of the Ca^{2+} regulation. We assume that increased Ca^{2+} levels at the motor site reduce active force generation by the motors ($p_1 < 0$).

The state diagram exhibits different regimes (Fig. 2). If the force f_{\max} is small, the motors are not strong enough to pull transduction channels open. In this case, the system is monostable with most of the channels closed. Increasing f_{\max} leads to channel opening. For intermediate forces and weak Ca^{2+} feedbacks, the system is bistable, i.e. open and closed channels coexist. For strong Ca^{2+} feedbacks, however, the motors can't sustain the forces required to maintain the channels open. Spontaneous oscillations occur in a region of both intermediate forces and feedback strengths. Note that there is no oscillation in the absence of Ca^{2+} feedback, i.e. for $S = 0$.

4. EFFECTS OF FLUCTUATIONS

Spontaneous hair-bundle oscillations are noisy.¹³ Noise terms η , η_a and δc in Eqns. 1-3 formally take into account the effects of various sources of fluctuations that destroy the phase coherence of hair-bundle movements. The stochastic forces η and η_a act respectively on X and X_a . The consequences of these forces have been analyzed for non-oscillating hair bundles.³² The fluctuations δc of the Ca^{2+} concentration in the stereocilia result from stochastic transitions between open and closed states of the transduction channels.³³ Noise terms are zero on average. Their strengths are characterized by autocorrelation functions $\langle \eta(t)\eta(0) \rangle$, $\langle \eta_a(t)\eta_a(0) \rangle$ and $\langle \delta c(t)\delta c(0) \rangle$ respectively. We assume that different noise sources are uncorrelated and that noise is Gaussian.

Assuming that the motors are deactivated ($f = 0$), we first discuss thermal contributions to the noise. The noise term η in Eq. 1 then results from brownian motion of fluid molecules which collide with the hair bundle and from thermal transitions between open and closed states of the transduction channels. By changing the

gating-spring extension, this channel clatter generates fluctuating forces on the stereocilia. The fluctuation-dissipation theorem implies that $\langle \eta(t)\eta(0) \rangle = 2k_B T \lambda \delta(t)$. The friction coefficient $\lambda = \lambda_h + \lambda_c$ results from two contributions: $\lambda_h \simeq 1.3 \cdot 10^{-7} \text{N}\cdot\text{s}\cdot\text{m}^{-1}$ accounts for hydrodynamic friction, which depends on bundle geometry and fluid viscosity,^{18,34} whereas λ_c results from channel clatter. The contribution λ_c can be estimated from the autocorrelation function of the force η_c that results from stochastic opening and closing of N transduction channels

$$\langle \eta_c(t)\eta_c(0) \rangle \simeq D^2 K_{\text{gs}}^2 P_o(1 - P_o) N^{-1} e^{-|t|/\tau_c} \simeq 2D^2 K_{\text{gs}}^2 P_o(1 - P_o) N^{-1} \tau_c \delta(t) \quad . \quad (5)$$

Assuming that $\langle \eta_c(t)\eta_c(0) \rangle \simeq 2k_B T \lambda_c \delta(t)$, we define a hair bundle friction λ_c which is associated to channel opening and closing. Using Eq. 5, we estimate

$$\lambda_c \simeq \frac{K_{\text{gs}}^2 D^2 P_o(1 - P_o) \tau_c}{N k_B T} \quad . \quad (6)$$

Using typical parameter values our estimate reveals that channel clatter dominates friction and $\lambda \simeq 3 \cdot 10^{-6} \text{N}\cdot\text{s}\cdot\text{m}^{-1}$.

The noise strength resulting from stochastic motor action can also be estimated. Measurements of the initial adaptation rate as a function of the magnitude of step stimuli³⁵ imply that $\lambda_a \simeq 1.3 \cdot 10^{-5} \text{N}\cdot\text{s}\cdot\text{m}^{-1}$. The stochastic activity of motors generates an active contribution η_m to η_a with

$$\langle \eta_m(t)\eta_m(0) \rangle \simeq \gamma^2 N_a p(1 - p) f^2 e^{-|t|/\tau_a} \simeq 2N_a \gamma^2 p(1 - p) f^2 \tau_a \delta(t) \quad . \quad (7)$$

Here we have assumed that the N_a motors fluctuate independently and that relevant time scales for a hair-bundle oscillation are longer than τ_a which is the characteristic time of force production by the motors. This noise strength can be described by introducing an effective temperature T_m defined by $\langle \eta_m(t)\eta_m(0) \rangle \simeq 2k_B T_m \lambda_a \delta(t)$. With $f \simeq 1 \text{pN}$, $\tau_a \simeq 10 \text{ms}$ and $p \simeq 0.05$, we find $T_m/T \simeq N_a \gamma^2 p(1 - p) f^2 \tau_a / (k_B T \lambda_a) \simeq 0.5$. Writing $\langle \eta_a(t)\eta_a(0) \rangle = 2k_B T_a \lambda_a \delta(t)$, we thus get $T_a \simeq 1.5T$. Finally, we can show that fluctuations in the Ca-concentration do not have a significant effect on the observed fluctuation of hair bundle motion and can be neglected.²⁸

5. LINEAR AND NONLINEAR RESPONSE FUNCTIONS

Fluctuations destroy the phase coherence of spontaneous oscillations and conceal the bifurcations between the dynamic states displayed in the state diagram. The response of a noisy oscillating system to a periodic force $F_{\text{ext}} = F_1 e^{-i\omega t} + F_1^* e^{i\omega t}$ thus behaves effectively as that of a stable system. The response function $\chi(\omega) = X_1/F_1$, where X_1 is the amplitude of the phase-locked response, can be described for small stimulus amplitude by

$$\chi_0(\omega) \simeq \frac{1}{2} \left(\frac{e^{-i\alpha}}{i\Lambda(\omega_0 - \omega) + K} + \frac{e^{+i\alpha}}{-i\Lambda(\omega_0 + \omega) + K} \right) \quad . \quad (8)$$

This response function is characterized by the stiffness K and the friction coefficient Λ . The phase α describes the phase lag of the bundle's displacement with respect to the stimulus at the characteristic frequency ω_0 .

Numerical simulations of Eqns. 1-3 allow us to calculate linear and nonlinear response functions of the system in the presence of periodic force stimuli, see Fig. 3.²⁸ The only free parameters are the feedback strength S and the maximal motor force f_{max} . Along a line of constant open probability P_o in the state diagram, we determined the parameters in Eq. 8 as a function of f_{max} in the presence of noise. For $P_o = 0.5$, the characteristic frequency of spontaneous oscillations varies between a few Hertz and about 50Hz in the range $f_{\text{max}} = 330 - 800 \text{pN}$ within which a peak was detected in the spectral density of spontaneous movements. If $\alpha \simeq 0$, the linear response function has the same shape as that observed experimentally,¹³ Therefore, we elected the value of the motor force $f_{\text{max}} \simeq 352 \text{pN}$ at which this condition was satisfied for $P_o = 0.5$. At this operating point, the system displayed noisy spontaneous oscillations $X(t)$ that are similar to the hair-bundle oscillations observed in the bullfrog's sacculus.

The calculated linear response function χ_0 as a function of frequency agrees quantitatively with the experimental observations.¹³ At the characteristic frequency of the spontaneous oscillations, the sensitivity $|\chi|$ of the system to mechanical stimulation exhibits the three regimes observed experimentally¹⁴ as a function of the

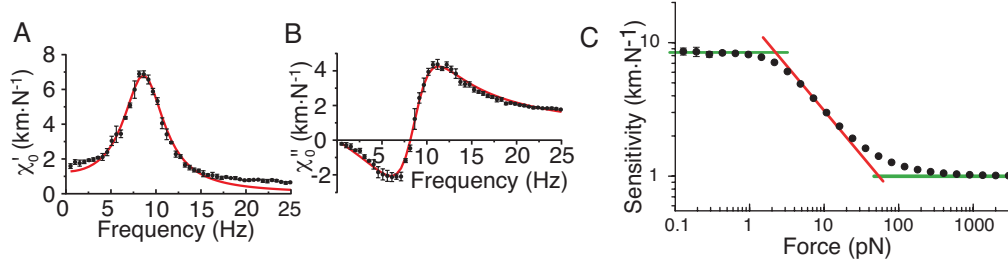


Figure 3. Response functions calculated from numerical simulation of the model equations with noise terms in presence of a periodic stimulus force. (A) Real part χ' of the linear response function. (B) Imaginary part χ'' of the linear response. (C) nonlinear response function at fixed frequency 8Hz.

stimulus amplitude $|F_1|$ (Fig. 3C): a linear regime of maximal sensitivity $|\hat{\chi}_0| = 8.5 \text{ km}\cdot\text{N}^{-1}$ at $\omega = \omega_0$ for small stimuli, a compressive nonlinearity for intermediate stimuli and a linear behavior of low sensitivity for large stimuli. The maximal sensitivity as well as the breadth of the nonlinear region are in quantitative agreement with experiments. An important parameter that influenced the system's maximal sensitivity is the stiffness of the load to which the hair bundle is coupled. For $f_{\text{max}} \simeq 352 \text{ pN}$, power spectra of spontaneous oscillations and response functions were not significantly affected by varying P_o in the range 0.2-0.8. Agreement between simulations and experiments thus did not qualify a particular value of P_o .

6. DISCUSSION

We have presented a physical description of active hair-bundle motility that emphasizes the role played by fluctuations. The mechanical properties of oscillatory hair bundles in the presence of a periodic stimulus force can be described quantitatively only if fluctuations are taken into account. Fluctuations arise in part from brownian motion of fluid molecules and from the stochastic gating of transduction channels. By consuming energy, the motors power frequency-selective amplification but also generate non-thermal fluctuations that add to the inevitable thermal fluctuations. We find, however, that the magnitude of fluctuations due to active processes remain below the level of thermal noise.

In the absence of fluctuations, an operating point on the line of Hopf bifurcations in the state diagram would result in diverging sensitivity, infinite frequency selectivity and a compressive nonlinearity over many decades of stimulus magnitudes. This situation is ideal for detecting oscillatory stimuli.^{7-9, 11, 36} As exemplified by our analysis, fluctuations restrict the system's sensitivity and frequency selectivity to oscillatory stimuli as well as the range of stimulus magnitudes over which the compressive nonlinearity of the bundle's response occurs. Despite fluctuations, a single hair bundle amplifies its response to small stimuli and, correspondingly, the characteristic compressive nonlinearity that arises near a Hopf bifurcation remains. One can define the gain of the amplificatory process as the ratio of the sensitivity at resonance to small stimuli $|\hat{\chi}_0|$ and that to intense stimuli. Both experiments and simulations indicate that active hair-bundle motility provides a gain of about ten. Our theoretical analysis demonstrates that significant amplification happens inside the area of the state diagram where the noiseless system oscillates. Interestingly, the global optimum of mechanosensitivity is obtained at an operating point located near the center of the oscillatory region in the state diagram, thus far from the line of Hopf bifurcations of the noiseless system. Furthermore, the sensitivity is largest if the open probability of the transduction channels is 0.5.

The ability of a single hair bundle to detect oscillatory stimuli using critical oscillations is limited by fluctuations which conceal the critical point. This limitation could be overcome if an ensemble of hair cells with similar characteristic frequencies were mechanically coupled. Coupled noisy oscillators could approach the ideal case of a critical oscillator near a Hopf bifurcation. In an intact mammalian cochlea, the gain that characterizes amplification of basilar-membrane motion is up to 10^3 ,¹⁰ which can be compared to a gain of only about 10 for a single hair bundle in the bullfrog's sacculus. This suggests that in the cochlea the effects of fluctuations of

individual hair cells could be reduced by the cooperative action of many oscillatory cells, whether the oscillations are provided by active hair-bundle motility or by a different mechanism.

We thank Thomas Duke, Martin Göpfert, Jim Hudspeth, and Jaques Prost for stimulating discussions.

REFERENCES

1. Hudspeth, A.J.: Nature (London) **341**, 397-404 (1989) .
2. Dallos, P., Popper A.N., and Fay R.R., *The cochlea* (Springer, New York) (1996).
3. Gold, T.: Proc. R. Soc. London Ser B **135** (1948).
4. Dallos, P.: J. Neurosci. **12**, 4575-4585 (1992).
5. Hudspeth A.J.: Curr. Opin. Neurobiol. **7**, 480-486 (1997).
6. Probst, R.: Adv. Otorhinolaryngol. **44**, 1-91 (1990).
7. Choe, Y., Magnasco, M., and Hudspeth A.J.: Proc. Natl. Acad. Sci. **95**, 15321-15326 (1998).
8. Camalet, S., Duke, T., Jülicher F., and Prost J.: Proc. Natl. Acad. Sci. **97**, 3183-3188 (2000).
9. Eguiluz, V.M., Ospeck, M., Choe Y., Hudspeth. A.J., and Magnasco, M.: Phys. Rev. Lett **84**, 5232-5235 (2000).
10. Ruggero, M.A., Rich, N.C., Recio, A., Narayan, S.S., and Robles, L.: J. Acoust. Soc. Am. **101**, 2151-2163 (1997).
11. Jülicher, F., Andor, D., and Duke, T.: Proc. Natl. Acad. Sci. **98**, 9080-9085 (2001).
12. Martin, P., and Hudspeth, A.J.: Proc. Natl. Acad. Sci. **96**, 14306-14311 (1999).
13. Martin, P., and Hudspeth A.J., and F. Jülicher: Proc. Natl. Acad. Sci. **98**, 14380-14385 (2001).
14. Martin, P., and Hudspeth, A. J.: Proc. Natl. Acad. Sci. **98**, 14386-14391 (2001).
15. Manley, G. A., Kirk, D. L., Koppl, C., and Yates, G. K.: Proc. Natl. Acad. Sci. **98**, 2826-2831 (2001).
16. Martin, P., and Hudspeth A.J.: Proc. Natl. Acad. Sci. **98**, 14386-14391 (2001).
17. Kachar, B., Parakkal, M., Kurc, M., Zhao, Y., and Gillespie, P.G. : Proc. Natl. Acad. Sci. **97**, 13336-13341 (2000).
18. Howard, J., and Hudspeth, A.J.: Neuron **1**, 189-199 (1988).
19. Fettiplace., R., Ricci, A.J., and Hackney, C.M.: Trends in Neurosci. **24**, 169-175 (2001).
20. Jülicher, F., and Prost, J.: Phys. Rev. Lett. **75**, 2618-2621 (1995).
21. Hudspeth, A. J., and Gillespie, P. G.: Neuron **12**, 1-9 (1994).
22. Benser, M. E., Marquis, R. E., and Hudspeth, A. J.: J. Neurosci. **16**, 5629-5643 (1996).
23. Wu, Y. C., Ricci, A. J., and Fettiplace, R.: J. Neurophysiol. **82**, 2171-2181 (1999).
24. Ricci, A. J., Crawford, A. C., and Fettiplace, R.: J. Neurosci. **20**, 7131-7142 (2000).
25. Vilfan, A., and Duke, T.: Biophys. J. **85**, 191-203 (2003).
26. Martin, P., Mehta, A., and Hudspeth, A.J.: Proc. Natl. Acad. Sci. **97**, 12026-12031 (2000).
27. Martin, P., Bozovic, D., Choe, Y., and Hudspeth, A. J.: J. Neurosci. **23**, 4533-4548 (2003).
28. Nadrowski, B., Martin, P., Jülicher, F.: Proc. Natl. Acad. Sci. **101**, 12195-12200 (2004).
29. Markin, V. S., and Hudspeth, A. J.: Annu. Rev. Biophys. Biomol. Struct. **24**, 59-83 (1995).
30. Strogatz, S. T.: (1997) *Nonlinear Dynamics and Chaos*. (Addison-Wesley, Reading, MA), 7th edition.
31. Lumpkin, E. A., and Hudspeth, A. J.: J. Neurosci. **18**, 6300-6318 (1998).
32. Frank, J. E., Markin, V., and Jaramillo, F.: Biophys. J. **83**, 3188-201 (2002).
33. van Netten, S. M., Dinklo, T., Marcotti, W., and Kros, C. J.: Proc. Natl. Acad. Sci. **100**, 15510-15515 (2003).
34. Denk, W., Webb, W. W., and Hudspeth, A. J. Proc. Natl. Acad. Sci. **86**, 5371-5375 (1989).
35. Hacohen, N., Assad, J. A., Smith, W. J., and Corey, D. P.: J. Neurosci. **9**, 3988-3997 (1989).
36. Duke, T., and Jülicher, F.: Phys. Rev. Lett. **90**, 158101 (2003).